Available online at www.sciencedirect.com
SCIENCE DIRECT®
Polymer 44 (2003) 3827–3835
polymer
www.elsevier.com/locate/polymer

# Synthesis, characterizations and properties of new copoly(aryl ether)s with alternate hole- and electron-transporting fluorophores

Yun Chen*, Shiao-Wen Hwang, Yun-Hao Yu

*Department of Chemical Engineering, National Cheng-Kung University, Tainan 701, Taiwan, ROC*

Received 9 January 2003; received in revised form 15 April 2003; accepted 18 April 2003

**Abstract**

Three novel copoly(aryl ether)s, consisting of alternate isolated hole-transporting (2,5-dihexyloxy-1,4-distyrylbenzene) and electron-transporting (*p*-quaterphenyl or aromatic 1,3,4-oxadiazole) segments, were synthesized from corresponding bis(phenol) and bis(fluoride) monomers by nucleophilic displacement reaction. These copolymers are soluble in common organic solvents and exhibit good thermal stability with 5% weight loss temperature above 400 °C in nitrogen atmosphere. The photoluminescent (PL) spectra and quantum yields of these copolymers are dependent on the composition of the isolated fluorophores. The HOMO and LUMO energy levels of these copolymers have been estimated from their cyclic voltammograms. All the observations directly proved that the oxidation in copolymers starts at the hole transporting segments. Moreover, the electron and hole affinities can be enhanced simultaneously by introducing isolated hole-transporting and electron-transporting segments, in which *p*-quaterphenyl is more electron-affinitive than aromatic 1,3,4-oxadiazole chromophores.


*Keywords:* Poly(aryl ether)s; Hole-transporting; Electron-transporting

## 1. Introduction

Recently, π-conjugated electroluminescent polymers have attracted much attention as the best candidate for flat panel displays after the discovery of light emission from poly(*p*-phenylenevinylene) (PPV) thin film sandwiched between an anode and a cathode electrode [1–4]. Many research groups have tried to improve the quantum efficiency and to synthesize short-wavelength light-emitting polymers for blue light [4–6].

The emitting wavelength is mainly determined by the effective π-conjugation length in the excited state and by non-resonant or resonant coupling to surrounding electronic oscillators [7]. The electroluminescence (EL) arises from radiative relaxation of excitons, which are formed by recombination of electrons and holes injected from the two opposite electrodes. To achieve high EL efficiency, it is necessary to balance the injection rates of opposite charges and decrease the barriers of charge injection from the opposite contacts [8]. Many conjugated polymers containing electron-transporting chromophores have been synthesized to reduce the barrier of electron injection, which is a key factor in balancing charges injection [9–12]. However, excess of conjugated length usually results in red-shifting the wavelength of photoluminescence (PL) and EL. The isolated polymers consisting of defined hole transporting (donor) or electron transporting (acceptor) segments are also interesting because the electron and hole affinities can be enhanced simultaneously, and the non-conjugated spacers can conduce to big band gap for blue emission [13–14].

In this work, three poly(aryl ether)s (see Scheme 1) consisting of alternate isolated hole-transporting/emitting segments (distyrylbenzene) derivative and electron-transporting segments (*p*-quaterphenyl or aromatic 1,3,4-oxadiazole) were synthesized and characterized. We attempted to balance the electron and hole affinities in these copolymers, and decrease charge injection barriers from the opposite electrodes simultaneously [15–17]. The optical and electrochemical properties of these poly(aryl ether)s have been investigated in detail. A conjugated polymer **P3** [18] is compared with the isolated polymer **P3** in optical and electrochemical properties.

* Corresponding author. Tel.: +886-6-2085843; fax: +886-6-2344496.
*E-mail address:* yunchen@mail.ncku.edu.tw (Y. Chen).

0032-3861/03/$ - see front matter © 2003 Elsevier Science Ltd. All rights reserved.
doi:10.1016/S0032-3861(03)00343-4

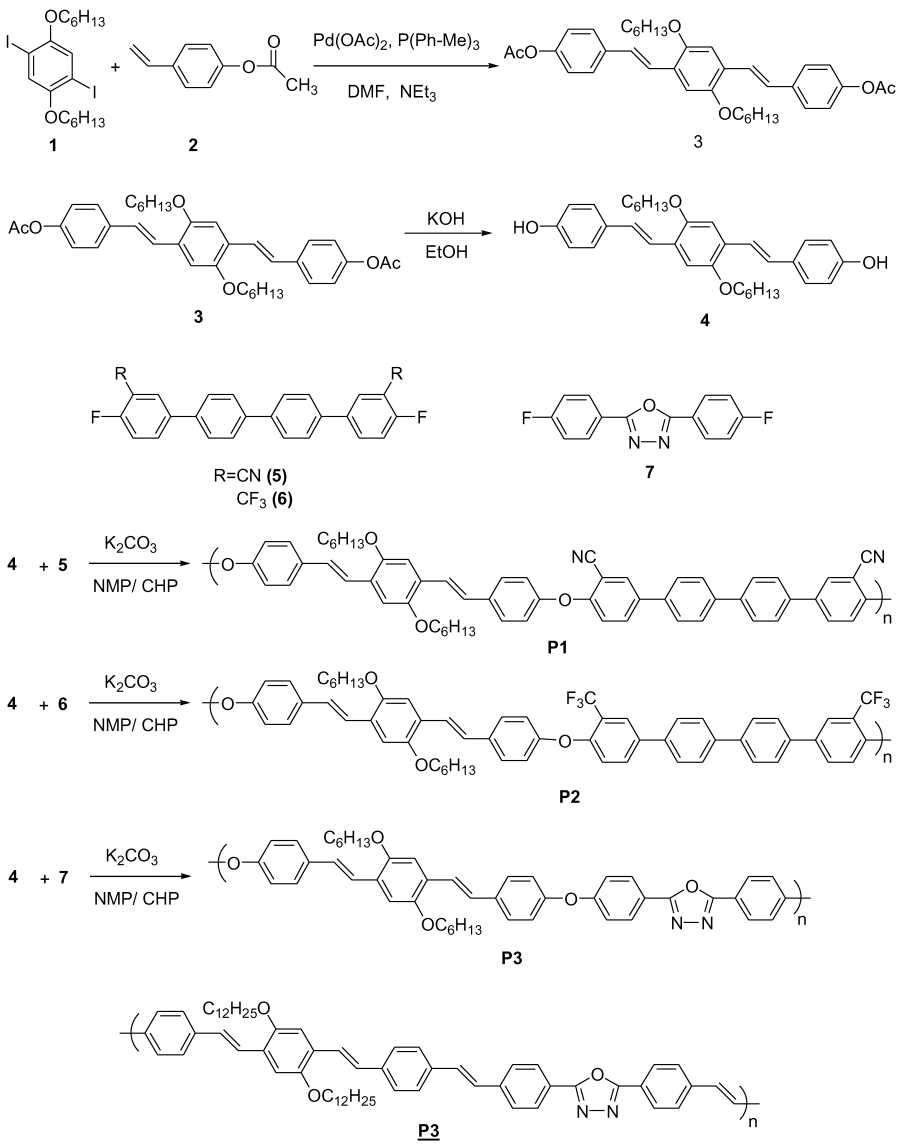


Scheme 1.

## 2. Experimental section

### 2.1. Materials and measurements

The synthetic procedures of monomers **1**, **5**, **6**, **7** [19–20] and model compounds [16–17] were analogous to that provided elsewhere. Triethylamine ($NEt_3$) was distilled over KOH. 4-Acetoxystyrene (Aldrich), palladium (II) acetate [$Pd(OAc)_2$, Acros], tri-(*o*-tolyl)phosphine [$P(Ph\text{-}Me)_3$, Acros] were used without further purification. Ethanol (Nasa), *N*,*N*-dimethylformamide (DMF, Tedia), *N*-methyl-2-pyrrolidone (NMP, Riedel-Dehaen), *N*-cyclohexyl-pyrrolidone (CHP, Janssen Chimica Co.), chloroform ($CHCl_3$, Tedia), tertrahydrofuran (THF, Tedia) and other solvents were HPLC grade reagents and used without any further purification. All new compounds were identified by $^1H$ NMR, FT-IR, and elemental analysis (EA). The $^1H$ NMR spectra were recorded on a Bruker AMX-400 MHz FT-NMR and chemical shifts are reported in ppm using tetramethylsilane (TMS) as an internal standard. The FT-IR spectra were measured as KBr disk on a fourier transform infrared spectrometer, model Valor III from Jasco. The EA was carried out on a Heraus CHN-rapid elemental analyzer. The thermogravimetric analysis (TGA) of the polymers was performed under nitrogen atmosphere at a heating rate of 20 °C/min using a Perkin–Elmer TGA-7 thermal analyzer. UV–Visible spectra were measured on Jasco V-550 spectrophotometer. The PL spectra were obtained using a Hitachi F-4500 fluorescence spectrophotometer. The diagrammatic curves of cyclic voltammetry were measured on BAS CV-50 W at room temperature under nitrogen atmosphere using ITO glass as working electrode, Ag/AgCl electrode as reference electrode and platinum wire electrode as auxiliary electrode supporting in 0.1 M $(n\text{-}Bu)_4NClO_4$ in acetonitrile. The energy levels were calculated using the

ferrocence (FOC) value of −4.8 eV with respect to vacuum level, which is defined as zero [21].

### 2.2. Monomer synthesis (Scheme 1)

#### 2.2.1. 1,4-Bis( p-acetoxystyryl)-2,5-dihexyloxybenzene (3)

Triethylamine (0.54 g, 5.30 mmol) was added to a solution of monomer **1** (0.90 g, 1.69 mmol), 4-acetoxystyrene **2** (0.83 g, 5.10 mmol), $Pd(OAc)_2$ (16 mg, 0.07 mmol), and $P(Ph\text{-}Me)_3$ (0.11 g, 0.36 mmol) in 7 ml of DMF. The mixture was stirred at 100 °C in a nitrogen atmosphere for 60 h. The reaction mixture was poured into distilled water, and extracted with chloroform. The extract was washed with distilled water, dried with anhydrous magnesium sulfate, filtered, and concentrated to give solid. The yellow product **3** was crystallized from 95% ethanol and from *n*-hexane/ethyl acetate thereafter. The yield was 66% (mp: 147–149 °C). $^1$H NMR (DMSO-$d_6$, ppm): 7.56 (d, 4H, aromatic H), 7.36 (s, 4H, vinyl H), 7.30 (s, 2H, aromatic H), 7.13 (d, 4H, aromatic H), 4.06 (t, 4H, $-OCH_2-$), 2.27 (s, 6H, $-CH_3$), 1.79 (t, 4H, $-CH_2-$), 1.49 (t, 4H, $-CH_2-$), 1.34 (t, 8H, $-CH_2-$), 0.87 (t, 6H, $-CH_3$). FT-IR (KBr pellet, $cm^{-1}$): 2934 (C–H), 2864, 1751 (C=O), 1508, 1422, 1368, 1255 (C–O–C), 1193, 1163, 1073, 1013 (C–O–C), 972 (*trans* –C=C–). Anal. calcd (%) for $C_{38}H_{46}O_6$: C, 76.22; H, 7.74. Found: C 76.05; H, 7.79.

#### 2.2.2. 1,4-Bis( p-hydroxystyryl)-2,5-dihexyloxybenzene (4)

A mixture of **3** (1.88 g, 3.13 mmol) and KOH (1.76 g, 31.4 mmol) in 30 ml ethanol was stirred at 80 °C in a nitrogen atmosphere for 4 h. After reaction was completely promoted, the reaction mixture was poured into 2 N HCl (400 ml). The yellow products **4** were filtered out and washed with a large amount of water and then dried in a vacuum oven. The yield was 99% (mp: 184–186 °C). $^1$H NMR (DMSO-$d_6$, ppm): 9.55 (s, 2H, OH), 7.35 (d, 4H, aromatic H), 7.20 (d, 6H, aromatic H and vinyl H), 6.76 (d, 4H, aromatic H), 4.03 (t, 4H, $-OCH_2-$), 1.78 (t, 4H, $-CH_2-$), 1.50 (t, 4H, $-CH_2-$), 1.34 (t, 8H, $-CH_2-$), 0.87 (t, 6H, $-CH_3$). FT-IR (KBr pellet, $cm^{-1}$): 3369 (O–H), 2929 (C–H), 2864, 1606, 1513, 1428, 1382, 1237 (C–O–C), 1209, 1173, 964 (*trans* –C=C–). Anal. calcd (%) for $C_{34}H_{42}O_4$: C, 79.34; H, 8.22. Found: C 79.20; H, 8.32.

### 2.3. Polymerization (Scheme 1)

The poly(aryl ether)s were prepared from bis(phenol) monomer (**4**) with *p*-quaterphenyl or 1,3,4-oxadiazole monomers (**5**–**7**) by the nucleophilic displacement reaction. For example, to a two-necked 25 ml glass reactor was charged with **4** (0.257 g, 0.50 mmol), **5** (0.196 g, 0.50 mmol), 10 ml solvent mixture of toluene/NMP/CHP (v/v/v = 2:1:1) and an excess of $K_2CO_3$ (0.166 g, 1.20 mmol). The reaction mixture was then stirred at 170 °C for 13 h, during which the toluene was removed by condensing in the Dean–Stark trap. The reaction mixture was diluted with 2 ml of NMP, and then dropped into 250 ml of methanol/distilled water (v/v = 2:1) solvent mixture. The appearing **P1** precipitates were collected by filtration and was further purified by extracting with a Soxhlet extractor for overnight using isopropyl alcohol as solvent. The conditions and results are given in Table 1.

#### 2.3.1. Poly[oxy[1,4-bis( p-styryl)-2,5-dihexyloxybenzene-oxy]-3,3‴-dicyano-p-quaterphenyl-4,4‴-ylene] (P1)

The polymer yield was 0.356 g (82.1%). $\eta_{red}$ = 0.83 dl/g. $^1$H NMR ($C_2D_2Cl_4$, ppm): 7.91 (s, 2H, aromatic H), 7.68–7.59 (d, 14H, aromatic H), 7.45–7.36 (s, 4H, vinyl H), 7.16–6.95 (d, 8H, aromatic H), 4.02 (t, 4H, $-OCH_2-$), 1.85 (t, 4H, $-CH_2-$), 1.50 (t, 4H, $-CH_2-$), 1.37 (t, 8H, $-CH_2-$), 0.89 (t, 6H, $-CH_3$). FT-IR (KBr pellet, $cm^{-1}$): 2969 (C–H), 2836, 2150 (C≡N), 1592, 1475, 1399, 1242 (C–O–C), 1151, 971 (*trans* –C=C–). Anal. calcd (%) for $C_{60}H_{54}N_2O_4$: C, 83.11; H, 6.28; N, 3.23. Found: C 81.53; H, 6.33; N, 3.46.

#### 2.3.2. Poly[oxy[1,4-bis( p-styryl)-2,5-dihexyloxybenzene-oxy]-3,3‴-bis-(trifluoromethyl)-p-quaterphenyl-4,4‴-ylene] (P2)

The polymer yield was 0.473 g (99.3%). $\eta_{red}$ = 2.37 dl/g. $^1$H NMR ($C_2D_2Cl_4$, ppm): 7.89 (s, 2H, aromatic H), 7.72–7.55 (d, 14H, aromatic H), 7.41–7.35 (s, 4H, vinyl H), 7.12–7.08 (d, 8H, aromatic H), 4.03 (t, 4H, $-OCH_2-$), 1.84 (t, 4H, $-CH_2-$), 1.49 (t, 4H, $-CH_2-$), 1.31 (t, 8H, $-CH_2-$), 0.85 (t, 6H, $-CH_3$). FT-IR (KBr pellet, $cm^{-1}$): 2939 (C–H), 2872, 1697, 1484, 1332, 1248 ($CF_3$), 1222 (C–O–C), 980 (*trans* –C=C–). Anal. calcd (%) for $C_{60}H_{54}F_6O_4$: C, 75.61; H, 5.71. Found: C, 76.82; H, 5.83.

#### 2.3.3. Poly[oxy[1,4-bis( p-styryl)-2,5-dihexyloxybenzene-oxy]-2,5-diphenyl-1, 3, 4-oxadiazole] (P3)

The polymer yield was 0.361 g (98.5%). $\eta_{red}$ = 0.47 dl/g. $^1$H NMR ($C_2D_2Cl_4$, ppm): 8.1 (d, 4H, aromatic H), 7.55 (d, 4H, aromatic H), 7.46–7.42 (s, 2H, vinyl H), 7.15–6.87 (d, 12H, aromatic H), 4.05 (t, 4H, $-OCH_2-$), 1.87 (t, 4H, $-CH_2-$), 1.55 (t, 4H, $-CH_2-$), 1.38 (t, 8H, $-CH_2-$), 0.91 (t, 6H, $-CH_3$). FT-IR (KBr pellet, $cm^{-1}$): 3037, 2930 (C–H), 2857, 1694, 1598 (–C=N–), 1488, 1420, 1243, 1203 (C–O–C), 1065, 1012, 964 (*trans* –C=C–). Anal. calcd (%) for $C_{48}H_{48}N_2O_5$: C, 78.66; H, 6.60; N, 3.82. Found: C, 76.24; H, 6.49; N, 4.12.

## 3. Results and discussion

### 3.1. Synthesis and characterization

We could obtain all of the intermediate compounds in high yield, and these compounds were well-characterized through the data from melting points, $^1$H NMR, FT-IR, and elemental analyses. A typical Heck reaction condition was applied to the synthesis of bis(acetoxy) monomer (**3**) [22].

Table 1
Polymerization results and characterization of **P1**–**P3**

| No. | Reaction temperature (°C) | Reaction time (h) | Yield (%) | $\eta_{red}$[a] (dl/g) | $M_n$[b] ($\times 10^4$) | $M_w$[b] ($\times 10^4$) | PDI[b] | $T_d$[c] (°C) |
|---|---|---|---|---|---|---|---|---|
| **P1** | 170 | 13 | 82.1 | 0.83 | 3.11 | 9.84 | 3.84 | 401 |
| **P2** | 170 | 12 | 99.3 | 2.37 | 3.10 | 8.19 | 2.64 | 404 |
| **P3** | 150 | 15 | 98.5 | 0.47 | 2.82 | 5.32 | 1.88 | 435 |

[a] Measured in 0.3 g/dl chloroform at 30 °C.
[b] $M_n$, $M_w$, and PDI of the polymers were determined by gel permeation chromatography using polystyrene standards in THF.
[c] The 5% weight loss temperatures.

The results of the $^1$H NMR and FT-IR spectra clearly indicate that the monomer structures are as proposed and that the major configuration of the vinylene unit is in the *trans* form. Heck reaction is a preferable method than Wittig coupling in forming vinylene linkage of high *trans* form and purity [23–24].

Three copoly(aryl ether)s (**P1**–**P3**) consisting of alternate isolated hole-transporting and electron-transporting segments were synthesized by the nucleophilic displacement reaction of bis(phenol) monomer (**4**) with bis(fluoride) monomers (**5**, **6**, **7**). The polymerization results and the characterization data of these polymers are shown in Table 1. All the synthesized polymers are highly soluble in common organic solvents such as tertrahydrofuran, chloroform, 1,1,2,2-tetrachloroethane, and so on. The number-average molecular weights ($M_n$) and the weight-average molecular weights ($M_w$) of the polymers, determined by gel permeation chromatography using polystyrene as standard, are $3.11 \times 10^4$, $3.10 \times 10^4$, $2.82 \times 10^4$ and $9.84 \times 10^4$, $8.19 \times 10^4$, $5.32 \times 10^4$ with dispersity indexes of 3.84, 2.64, and 1.88 for **P1**, **P2**, and **P3**, respectively. The reduced viscosity of **P2** (2.37 dl/g) is much higher than that of **P1** (0.83 dl/g), which may be explained by much stronger intermolecular interactions in **P2** due to the presence of cyano groups. The polymers were well identified by $^1$H NMR (as shown in Fig. 1) and FT-IR.

Thermal characterization of the copoly(aryl ether)s was accomplished by TGA and differential scanning calorimetry (DSC). We were not able to detect the glass transitions for these polymers up to 300 °C by DSC. In TGA analyses, the weight losses were less than 5% on heating to 400 °C for each polymer.

### 3.2. Optical properties

The absorption and PL spectra of model compounds (as shown in Scheme 2), simulated the isolated fluorophores in our polymers, in chloroform solutions are shown in Fig. 2. Emitting and hole-transporting model **M1** shows the maximum PL peak at 444 nm, whereas those of electron-transporting models **M2**, **M3**, and **M4** locate at 380, 380, and 360 nm, respectively. The absorption and PL spectra of **P1**, **P2**, and **P3** in chloroform solutions are shown in Fig. 3(a) and the related data are listed in Table 2. The absorption spectra of the polymers all exhibit two broad peaks around 330 and 400 nm, which are attributed to electron- and hole-transporting segments, respectively.

The PL spectra of these polymers are very similar in shape, and all exhibit maximum PL peak at 450 nm although they contain different electron-transporting segments. Therefore the PL spectra of these poly(aryl ether)s in chloroform solution are dominated by the fluorophores with longer emissive wavelength. In order to confirm these phenomena, **M1** was blended with **M4** in the ratio of 1:1 in $5 \times 10^{-7}$ M chloroform solutions to simulate **P3** in $1 \times 10^{-6}$ M chloroform solution (as shown in Fig. 4). The PL spectra of blending solution was additive emission of **M1** (PL $\lambda_{max} = 444$ nm) with **M4** (PL $\lambda_{max} = 360$ nm). Moreover, the relative peak intensity at $\lambda_{max} = 360$ nm is reduced significantly when the excited wavelength increase from 300 to 330 nm, whereas that at $\lambda_{max} = 444$ nm shows an opposite trend. This is attributable to reduced absorbance of **M4** with increasing excitation wavelength from 300 to 330 nm (see Fig. 2). In the blending solution, there are no chemical bonding between the energy donor **M4** and the energy acceptor **M1**, and the distance between molecules is large (about 2500 Å). Therefore, the radiative transfer (reabsorption) is the major energy transfer route. However, for **P3** only the peak around $\lambda_{max} = 450$ nm can be observed in solution, and the peak at $\lambda_{max} = 360$ nm disappears completely. From the above-mentioned fact that radiative transfer from **M4** to **M1** is an incomplete process, there should exist a specified intrachain energy transfer in the polymer. The energy transfer in this donor-bridge-acceptor system was probably the result of the tunneling by electrons and holes [25]. Electrons and holes tunnel between the short bridge distance, and unlike hopping model they did not occupy the energy levels of LUMO and HOMO [26]. This tunneling model also could preserve the high relative quantum yield ($\Phi_{PL}$) in the polymers. The relative quantum yields ($\Phi_{PL}$), which were calculated from the corrected PL spectra, of **M1** in chloroform solution is 0.57, and those of **P1**, **P2**, and **P3** in solution are 0.51, 0.54, and 0.54, respectively.

The PL spectra of **P1**–**P3** in thin films show slight red-shifts (about 12 nm) and are characteristically broader compared to those of solution spectra (Fig. 3 and Table 2). These red-shifts are due to intermolecular $\pi-\pi$ interactions between the chromophores.

The **P3** with $\pi$-conjugated backbone is compared

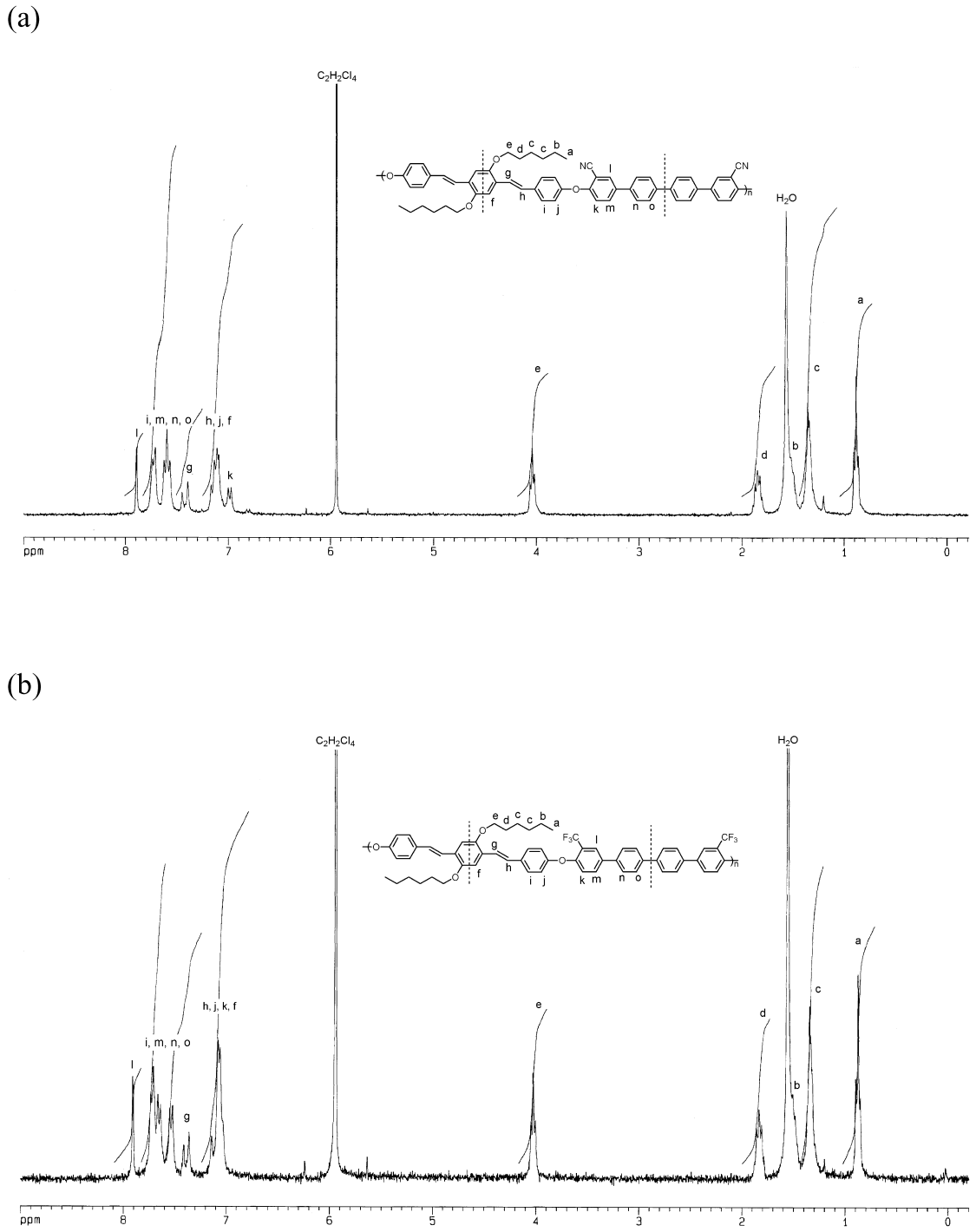


Fig. 1. $^1$H NMR spectra of (a) **P1**, (b) **P2** and (c) **P3**.

with **P3** containing isolated chromophores, and the optical data are shown in Fig. 5 and Table 2. The absorption maxima of **P3** ($\lambda_{max} = 442$ and 459 nm in $CHCl_3$ and as thin film, respectively) show a significant bathochromic shift as compared to those of **P3** ($\lambda_{max} =$ 400 and 401 nm in $CHCl_3$ and as film, respectively). The PL spectra exhibit similar trends (**P3**: $\lambda_{max} = 515$ and 550 nm in $CHCl_3$ and as thin film, respectively, as compared to **P3**: $\lambda_{max} = 452$ and 463 nm). Extension of conjugation length in **P3** results not only in narrower band gap but also much more flat molecular structure. The flat structure enhances aggregation in film state by $\pi-\pi$ stacking. It seems likely that both narrower band gap and aggregation in **P3** contribute to large red shifts in both absorption (58 nm) and PL spectra (87 nm) as compared to isolated **P3**. Moreover, lower quantum

(c)

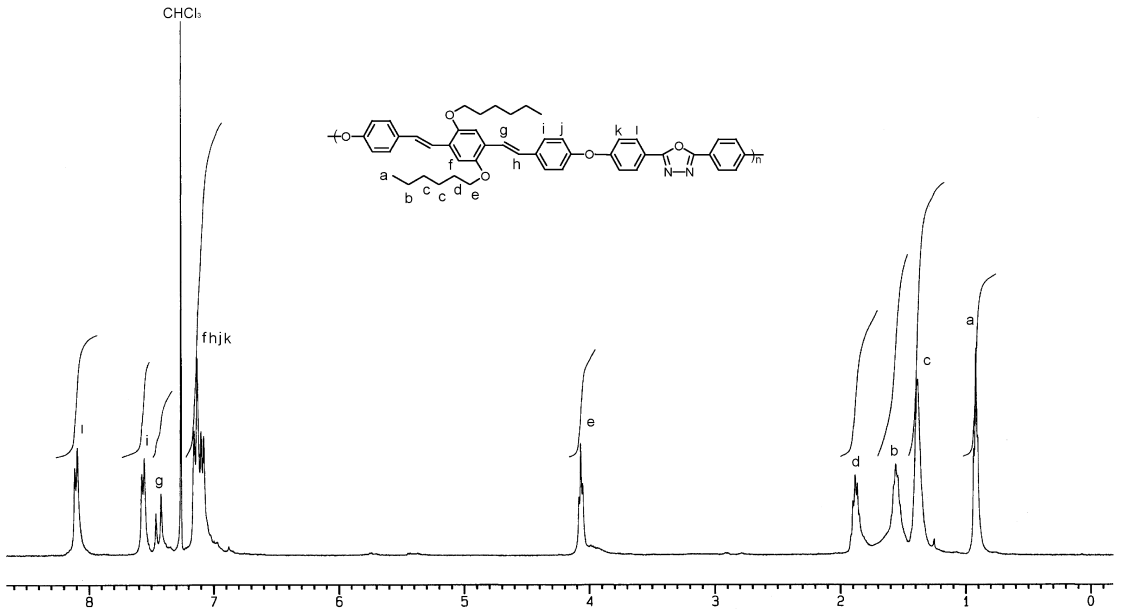


Fig. 1 (*continued*)

Table 2
Optical properties of the polymers

| No. | UV–Vis $\lambda_{max}$ [a] solution (nm) | UV–Vis $\lambda_{max}$ film (nm) | PL $\lambda_{max}$ [a] solution (nm) | PL $\lambda_{max}$ film (nm) | $\Phi_{PL}$ [b] solution |
|---|---|---|---|---|---|
| **P1** | 325, 400 | 332, 407 | 452, 475[s] | 465, 486[s] | 0.51 |
| **P2** | 324, 399 | 329, 403 | 450, 473[s] | 462, 482[s] | 0.54 |
| **P3** | 330, 400 | 328, 401 | 452, 475[s] | 463, 483[s] | 0.54 |
| **P3** | 362, 442 | 382, 459 | 515, 547[s] | 550 | 0.40 |

[a] $1 \times 10^{-5}$ M in $CHCl_3$. Superscript s means the wavelength of the shoulder.

[b] These values were estimated by using quinine sulfate (dissolved in 1N $H_2SO_{4(aq)}$ with a concentration of $10^{-5}$ M, assuming $\Phi_{PL}$ of 0.55) as a standard. The excitation wavelengths were 320 and 365 nm for **P1**–**P3** and **P3** solutions ($10^{-6}$ M repeating unit), respectively, which had absorbance of less than 0.05.

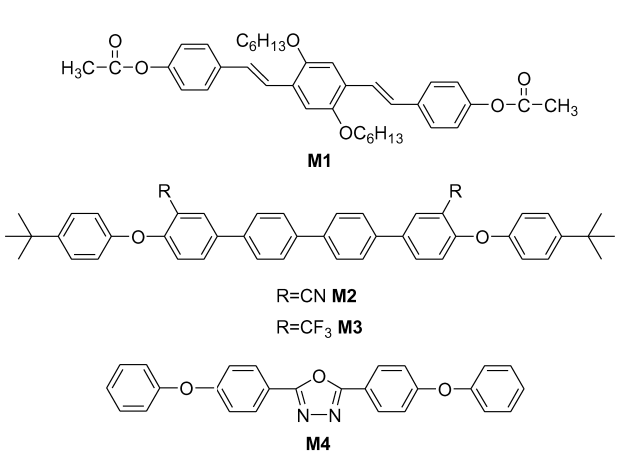


Scheme 2.

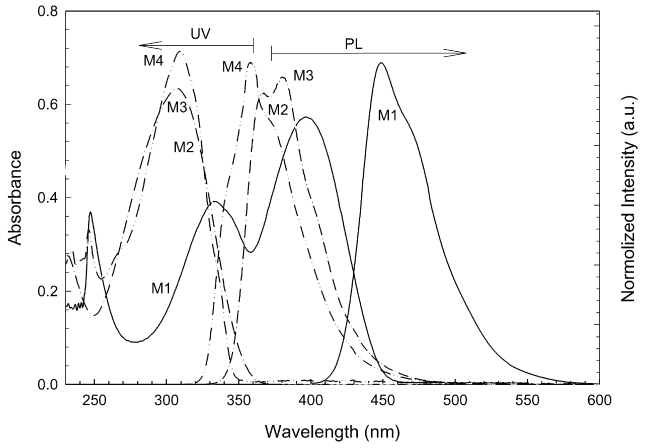


Fig. 2. Photoluminescence (excitation at 320 nm) and UV–Vis absorption spectra of **M1** (—), **M2** (– – –), **M3** (–·–·–) and **M4** (–··–··–) in $CHCl_3$ solutions of $1 \times 10^{-5}$ M.

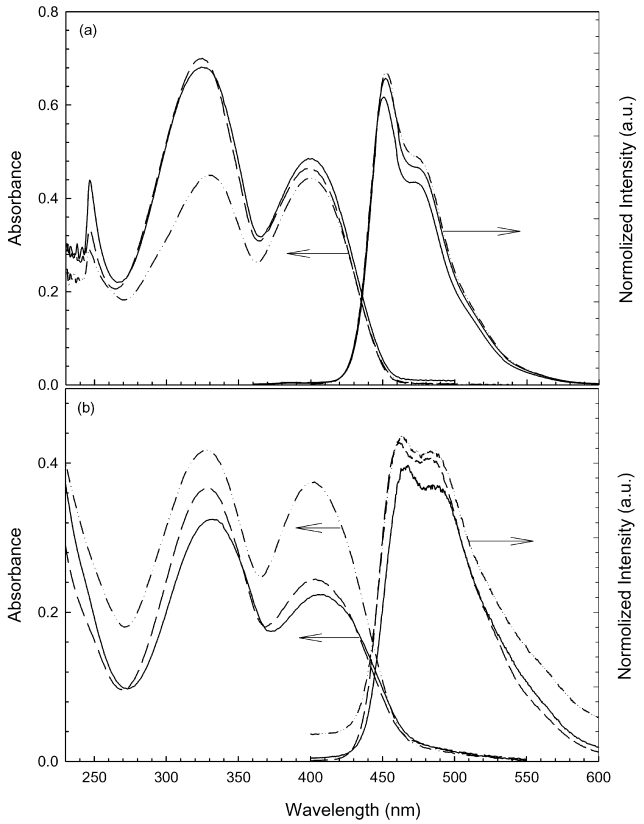


Fig. 3. Photoluminescence and absorption spectra of **P1** (—), **P2** (– – –), and **P3** (–··–··–) in $CHCl_3$ solutions of $1 \times 10^{-5}$ M (a) and films coated on quartz plate (b).

yield ($\Phi_{PL} = 0.40$) is also an unavoidable consequence of aggregation in solid state.

### 3.3. Electrochemical property

Typical cyclic voltammograms (CVs) of **P1**, **P2**, and **P3** in anodic scan are shown in Fig. 6. The onset oxidation potentials of **P1**, **P2**, and **P3** which have the same

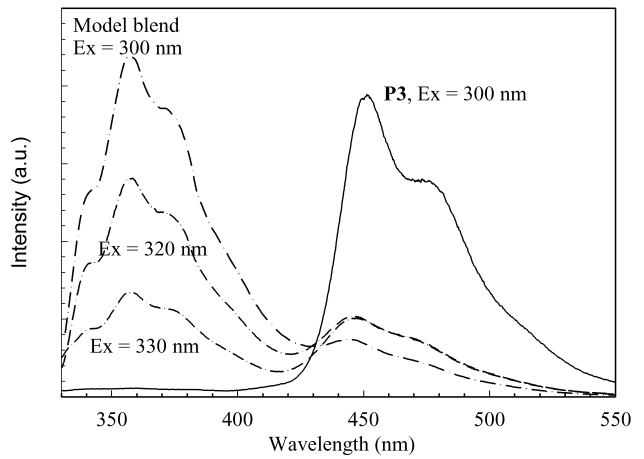


Fig. 4. The PL spectra of **P3** in $1 \times 10^{-6}$ M $CHCl_3$ solution and **M1/M4** = 1:1 blend in $5 \times 10^{-7}$ M $CHCl_3$ solutions. Ex: excitation wavelength.

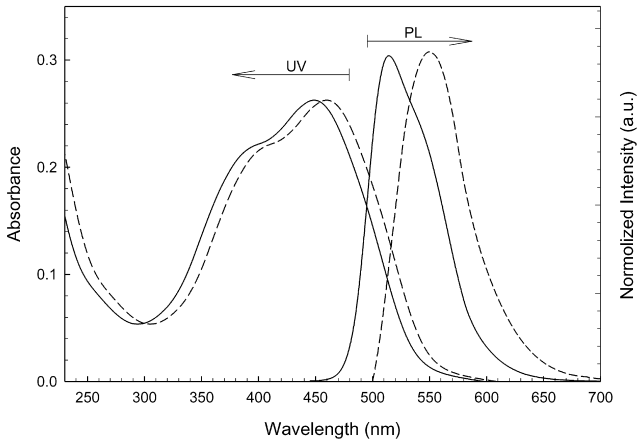


Fig. 5. Photoluminescence and absorption spectra of **P3** in $1 \times 10^{-5}$ M $CHCl_3$ solutions (—) and as film coated on quartz plate (– – –).

distyrylbenzene segments are almost the same and locate at 0.37 V, although they possess different electron-transporting segments. However, the oxidation onset potentials of electron-transporting model compounds (**M2**: 2.11 V, **M3**: 2.08 V, **M4**: 1.18 V) [16–17] are much greater than the corresponding polymers. The observations directly proved that the oxidation started at the hole-transporting segments. Identically, we could presume that the reduction would start at the electron-transporting segments. Therefore, for isolated poly(aryl ether)s with alternate hole- and electron-transporting segments, the band gaps estimated directly from the CV curves would be underestimated values (Fig. 7: overlapping part of solid and broken squares).

The HOMO and LUMO levels of the copoly(aryl ether)s can be calculated from the onset potentials (oxidation in anodic scan and reduction in cathodic scan) [27]. And the band gaps ($E_g^{opt}$) of model compounds, calculated from the onset wavelength of their absorption spectra, are 2.79, 3.51, 3.49, and 2.53 eV for **M1**, **M2**, **M3**, and **M4**, respectively. Therefore, the band structures of hole-transporting segment in the copoly(aryl ether)s can be constructed from their HOMO level and the band gap ($E_g^{opt}$) of the corresponding

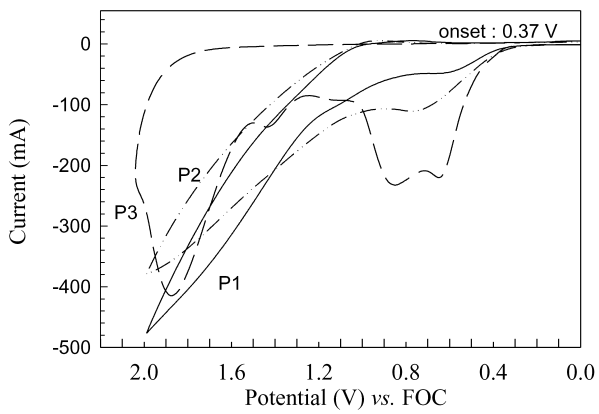


Fig. 6. Cyclic voltammograms of **P1** (—), **P2** (– – –), and **P3** (–··–··–) (100 mV/s) in coated on ITO glass electrode immersed in $CH_3CN$ solution of $Bu_4NClO_4$ (0.1 M).

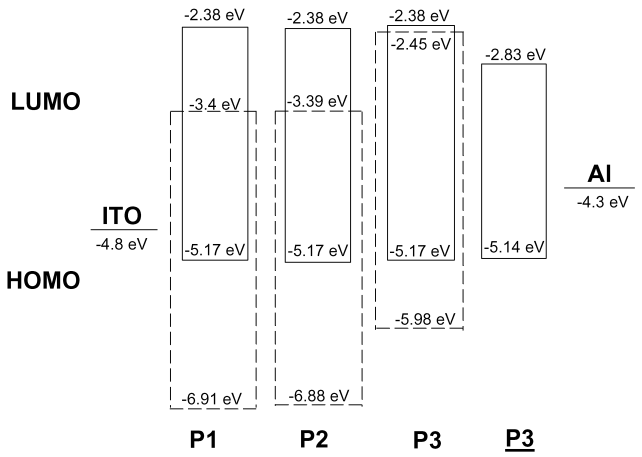


Fig. 7. Energy band diagram of **P1**–**P3** (hole-transporting segments (—); electron-transporting segments (- - -)) and **P3**.

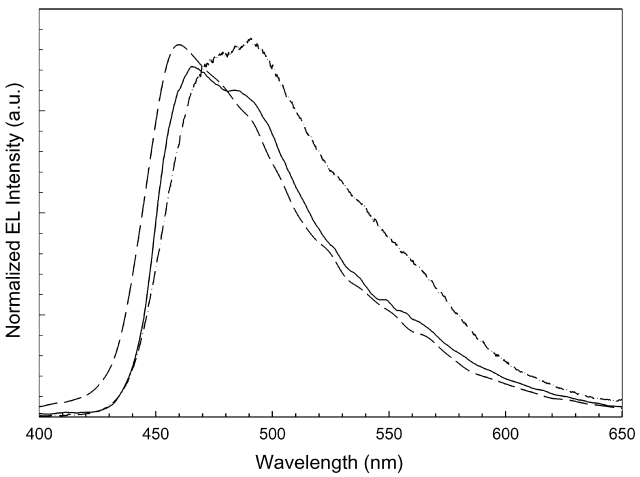


Fig. 8. Electroluminescence spectra of the single layer devices: ITO/**P1**/Al (—), ITO/**P2**/Al (– – –), and ITO/**P3**/Al (–·–·–).

hole-transporting model compounds (solid square). For example, the HOMO level of distyrylbenzene segment in **P1** is −5.17 eV and the LUMO is estimated to be −2.38 eV from the band gap of **M1** (2.79 eV). Similarly, the band structure of the electron-transporting segments can be constructed from their LUMO levels and the band gaps ($E_g^{opt}$) of the corresponding electron-transporting model compounds (broken square). Accordingly, the electrochemically determined band structures of the polymers are the overlapping region between their hole- and electron-transporting constitutional segments. It is noteworthy that the electron-injection barriers are reduced due to incorporation of electron-transporting segments, and the quaterphenyl chromophores (in **P1** and **P2**) are much more effective than oxadiazole (in **P3**) units in enhancing the electron affinity.

As mentioned above, the band gap of conjugated polymer **P3** was smaller than that of isolated poly(aryl ether) **P3** because of extended conjugation length. Moreover, the band structure of **P3** is integrated into single HOMO and LUMO levels. However, the isolated hole- and electron-transporting fluorophores in these poly(aryl ether)s function as hole and electron trap centers, the hole and electron are difficult to recombine as exciton. Thus, the carrier-hopping and carrier-tunneling barrier between the hole- and electron-transporting fluorophores is a specific factor to influence the exciton formation [18]. The single-layer LED devices, ITO/polymer/Al, have been fabricated and the electroluminescent spectra are shown in Fig. 8, which is basically consistent with the PL spectra, except **P3**. The detail of their optoelectronic properties are now under progress.

## 4. Conclusion

Three new poly(aryl ether)s consisting of alternate emissive/hole-transporting distyrylbenzene derivative and electron-transporting chromophores (quarterphenyl or aromatic 1,3,4-oxadiazole) have been successfully synthesized, and their photoluminescent and electrochemical properties have also been studied in detail. These isolated poly(aryl ether)s exhibit good thermal stability and are soluble in common organic solvent. For this kind of isolated copoly(aryl ether)s, the wavelengths of emission light are mainly attributed to distyrylbenzene segments due to effective energy transfer. Furthermore, the hole and electron affinities of the isolated copoly(aryl ether)s can be promoted simultaneously by introducing hole and electron transporting segments. Unfortunately, the recombination of hole and electron may be inhibited by the barrier between the two segments which were separated by oxygen.

## Acknowledgements

The authors thank the National Science Council of the Republic of China for financial aid through project NSC 90-2216-E006-036.

## References

[1] Burroughes JH, Bradley DDC, Brown AR, Marks RN, Mackay K, Friend RH, Burn PL, Holmes AB. Nature 1990;347:539.
[2] Braun A, Heeger AJ. J Appl Phys Lett 1991;58:1982.
[3] Kang IN, Hwang DH, Shim HK, Zyung T, Kim JJ. Macromolecules 1996;29:165.
[4] Kraft A, Grimsdale AC, Holmes AB. Angew Chem Int Ed 1998;37:402.
[5] Greenham NC, Moratti SC, Bradley DDC, Friend RH, Holmes AB. Nature 1993;365:628.
[6] Sokolik I, Yang Z, Karasz FE, Morton DCJ. Appl Phys Commun 1993;75:3584.
[7] Oelkrug D, Tompert A, Gierschner J, Egelhaaf HJ, Hanack M, Hohloch M, Steinhuber EJ. Phys Chem B 1998;102:1902.
[8] Greenham NC, Moratti SC, Bradley DDC, Friend RH, Holmes AB. Nature 1993;365:628.

[9] Peng Z, Bao Z, Galvin ME. Adv Mater 1998;10:680.
[10] Song SY, Jang MS, Shim HK, Song IS, Kim WH. Synth Met 1999; 102:1116.
[11] Chen ZK, Meng H, Lai YH, Huang W. Macromolecules 1999;32: 4351.
[12] Lee DW, Kown KY, Jin JI, Park Y, Kim YR, Hwang IW. Chem Mater 2001;13:565.
[13] Zheng M, Sarker AM, Gurel EE, Lahti PM, Karasz FE. Macromolecules 2000;33:7426.
[14] Zheng M, Ding L, Gurel EE, Lahti PM, Karasz FE. Macromolecules 2001;34:4124.
[15] Bredas JL, Heeger AJ. Chem Phys Lett 1994;217:507.
[16] Hwang SW, Chen Y. Macromolecules 2001;34:2981.
[17] Hwang SW, Chen Y. Macromolecules 2002;35:5438.
[18] Chen Y, Sheu RB, Wu TY. J Polym Sci Part A: Polym Chem 2003;41: 725.
[19] Bao Z, Chen Y, Cai R, Yu L. Macromolecules 1993;26:5281.
[20] Oberski J, Festag R, Schmidt C, Lussem G, Wendorff JH, Greiner A. Macromolecules 1995;28:8676.
[21] Liu Y, Liu MS, Jen AKY. Acta Polym 1999;50:105.
[22] Heck RF. Acc Chem Res 1979;12:146.
[23] Kim HK, Ryu MK, Kim KD, Lee SM, Cho SW, Park JW. Macromolecules 1998;31:1114.
[24] Ahn T, Shim HK. Macromol Chem Phys 2001;202:3180.
[25] McCommell HM. J Chem Phys 1961;35:508.
[26] Todd MD, Nitzan A, Ratner MA. J Chem Phys 1993;97:29.
[27] Liu Y, Liu MS, Jen AKY. Acta Polym 1999;50:105.